Iguratimod ameliorates rheumatoid arthritis progression through regulating miR-146a mediated IRAK1 expression and TRAF6/JNK1 pathway: an *in vivo* and *in vitro* study

R. Kong, J. Gao, L. Ji, Y. Peng, J. Zhang, D. Zhao

Department of Rheumatology and Immunology, Changhai Hospital, Naval Medical University, Shanghai, China.

Abstract

Objective

This study aimed to evaluate the therapeutic effect of iguratimod and its regulatory role on microRNA (miR-146a) and the downstream genes in treating rheumatoid arthritis-fibroblast-like synoviocytes (RA-FLS) and collagen-induced arthritis (CIA) rat model.

Methods

RA-FLS was isolated from knee synovial tissue of an active RA patient. In vitro, the effect of miR-146a mimic/inhibition on RA-FLS functions was investigated. Then the effect of Iguratimod on cell viability, proliferation, apoptosis, migration, invasion, inflammatory cytokines, miR-146a and its downstream gene/pathway in RA-FLS was evaluated. In vivo, the collagen induced arthritis (CIA) rat model was constructed, then the effects of iguratimod, miR-146a inhibition and their combination on treating CIA rat were assessed.

Results

Iguratimod treatment increased miR-146a while decreased cell proliferation, IRAK1 and TRAF6/JNK1 pathway in RA-FLS in a dose-dependent manner. Notably, iguratimod treatment repressed cell proliferation, migration, invasion, TNF-α, IL-1β, IL-6, IL-17, IRAK1 and TRAF6/JNK1 pathway in RA-FLS, while miR-146a inhibition alleviated the abovementioned effects of Iguratimod on RA-FLS. The in vivo experiments disclosed that iguratimod reduced systemic arthritis score, and decreased TNF-α, IL-1β, IL-6, IL-17, IRAK1 as well as TRAF6/JNK1 pathway, while enhanced apoptosis in synovial tissue of CIA rat model; and in miR-146a inhibition treated CIA rat model, the effect of iguratimod was diminished.

Conclusion

Iguratimod ameliorates RA progression via regulating miR-146a mediated IRAK1 expression and TRAF6/JNK1 pathway.

Key words

iguratimod, rheumatoid arthritis, microRNA-146a, rheumatoid arthritis-fibroblast-like synoviocytes, collagen-induced arthritis rat

*Ruina Kong, MM**
*Jie Gao, MD**
Lianmei Ji, MM
Yangxizi Peng, MM
Ju Zhang, MM
Dongbao Zhao, MD

**These authors contributed equally.*

Please address correspondence to:
Dongbao Zhao,
Department of Rheumatology and Immunology, Changhai Hospital, Naval Medical University, 168 Changhai Road, Yangpu District, Shanghai 200433, China
E-mail: dongbaozhao@163.com

Received on December 23, 2019, accepted in revised form on April 7, 2020.

Competing interests: none declared.

Introduction

Rheumatoid arthritis (RA), a disease not only damages the joints but also affects other organs or tissues, is a chronic inflammatory and autoimmune disease which causes a large physical, social and mental burden in patients (1). Swollen joint is the most common pathological change of RA, which is caused by the infiltration of leucocytes infiltration that is mediated by multiple cytokines and chemokines in the synovial tissue (2, 3). Preventing disease progression, joint damage and irreversible disability are the most crucial treatment aims. To achieve these aims, non-steroidal anti-inflammatory drugs (NSAIDs) and disease-modifying anti-rheumatic drugs (DMARDs) are widely applied in the clinical setting (1). Among all the therapeutics, DMARDs are the only ones which could prohibit the progression of joint damage, and the development of novel and effective DMARDs, especially the biological DMARDs and small-molecule kinase inhibitors, has contributed a lot to the improvement of RA patients' prognosis (4).

Iguratimod (also known as T614), a novel kind of DMARDs that is now generally used for RA treatment in China and in several other countries of East Asia, is an inhibitor of multiple immunoglobulins and cytokines, presenting with the effect of reducing inflammation, balancing immunity, and more importantly, protecting the bones (5). Although iguratimod is still a new drug for RA treatment, the number of studies assessing its treatment efficiency and safety is growing fast with time due to the favourable efficacy of iguratimod. For instance, mounting studies report that iguratimod is effective in decreasing disease activity and inflammation, besides, the rate of adverse events (AEs) caused by iguratimod is low (6-8). However, more efforts are needed to evaluate other detailed mechanisms of iguratimod in treating RA, since RA is a heterogeneous disease with intricate aetiology. Moreover, the increased findings regarding the detailed mechanisms of iguratimod in treating RA could also enhance the efficacy of combination use of iguratimod with other drugs that will ultimately improve the prognosis of RA patients.

MicroRNAs (miRNAs) are a category of tiny non-coding RNAs with a length of approximately 19-25 nucleotides, which present with the function of modulating the targeted gene(s) at the post-transcriptional level (9, 10). MiR-146a, a miRNA that regulates inflammation and immunity, is found to be expressed in human synovial tissue and present with protective effect on RA progression (11-15). For instance, in terms of inflammation, a prior study reveals that miR-146a alleviates kidney injury in an animal model of systemic lupus erythematosus via mediating nuclear factor-kappa B (NF-κB) pathway (16). As for immunity regulation, a study elucidates that miR-146a reduces inflammation by repressing innate immune response in atopic dermatitis (17). More interestingly, miR-146a is found to repress the expression of macrophage migration inhibitory factor (MIF), meanwhile, iguratimod is an inhibitor of MIF as reported by a previous study (18). However, no study has been conducted to assess the role of miR-146a in the therapeutic effect of iguratimod on treating RA.

Therefore, in this study, we aimed to investigate the effect of iguratimod on miR-146a and its downstream genes, as well as their interaction in treating RA-fibroblast-like synoviocytes (RA-FLS) and collagen-induced arthritis (CIA) rat model.

Methods

Cell culture

The RA-FLS was isolated from the knee synovium tissue of an active RA patient with swollen knee joint, and the control FLS (Ctrl-FLS) was separated from the knee synovium tissue derived from a non-arthritis (excluding RA, osteoarthritis, and so on) patient who underwent surgery due to knee trauma. The isolation procedures of FLS were performed according to the method described in our previous studies (19, 20). Then the FLS isolation was confirmed by viewing pure FLS under a microscope after three cell passages. This study was approved by the Ethics Committee of our hospital, and the informed consent was signed by patients. After

isolation, the cells were cultured in the DMEM medium (Gibco, USA) containing 10% fetal bovine serum (FBS). And the culture was performed at 37°C in the atmosphere of 5% CO_2 and 95% air. To evaluate the expression of miR-146a in RA-FLS and Ctrl-FLS, reverse transcription-quantitative polymerase chain reaction (RT-qPCR) was carried out. In addition, the RA-FLS from passage 3 to passage 8 were used for all the *in vitro* experiments.

Plasmids transfection and subsequent detection

MiR-146a mimic and NC mimic were respectively cloned into pGCMV-EGFP-miR-Blasticidin vector to construct miR-146a overexpression plasmid and NC overexpression plasmid. And miR-146a inhibitor and NC inhibitor were separately cloned into pRI-CMV-GFP-miRNA vector to construct the miR-146a inhibitor plasmid and NC inhibitor plasmid. All plasmids constructions were performed by Shanghai GenePharma Co., Ltd (Shanghai, China). These plasmids were transfected into RA-FLS using HlilyMax (Dojindo, Japan), and the cells were termed as Mimic-miR-146a cells, Mimic-NC cells, Inbibitor-miR-146a cells and Inhibitor-NC cells, correspondingly. The subsequent detections were carried out after transfection: RT-qPCR was performed to detect the miR-146a expression at 24 hour (h); Cell Counting Kit-8 (CCK-8) (Dojindo, Japan) was applied to assess the cell proliferation at 0h, 24h, 48h and 72h according to the manufacturer's instruction; Annexin V-FITC Apoptosis Detection Kit (BD, USA) was used to evaluate the cell apoptosis at 48h in terms of kit protocol; scratch wound healing assay was conducted to determine the cell migration ability at 48h; Transwell assay was carried out to assess the cell invasion ability at 48h; Meanwhile, the cell supernatant was collected at 48h, and enzyme-linked immunosorbent assay (ELISA) kits (Invitrogen, USA) was applied to measure the levels of tumour necrosis factor α (TNF-α), interleukin 1β (IL-1β), IL-6 and IL-17 in strict accordance with manufacturer's manual. Besides, the sensitivity for detecting the inflammatory cytokines in ELISA were (7.8-500 pg/mL, 2.3pg/mL) for TNF-α, (3.9-250pg/mL, 0.03pg/mL) for IL-1β, (10.24-400 pg/mL, <1 pg/mL) for IL-6 and (15-1000 pg/mL, 15-1000 pg/mL) for IL-17.

Assessment of pathway regulated by miR-146a

In the previous studies (21-23), miR-146a attenuates inflammation-induced activation of c-Jun NH2-terminal kinase 1 (JNK1) by directly targeting IL-1 receptor associated kinase 1 (IRAK1) and TNF receptor associated factor 6 (TRAF6) in human adipocytes. It is also found that the miR-146a could alleviate lipopolysaccharide-induced activation of hepatic stellate cell through inhibiting TRAF6-mediated JNK phosphorylation. Consequently, we assumed that miR-146a might be involved in the regulation of RA-FLS activity through IRAK1 and TRAF6/JNK1 pathway. As a result, the mRNA expressions of IRAK1, TRAF6 in mimic-miR-146a cells, mimic-NC cells, inbibitor-miR-146a cells and inhibitor-NC cells were detected by RT-qPCR at 48h post transfection, and the protein expressions of IRAK1, TRAF6, JNK1 and phosphorylation-JNK 1 (p-JNK1) in mimic-miR-146a cells, mimic-NC cells, inbibitor-miR-146a cells and inhibitor-NC cells were detected by western blot at 48h post transfection.

Iguratimod (T614) treatment for RA-FLS

RA-FLS was treated with iguratimod (T614) (Sigma, USA) at different concentrations (0, 5, 10, 20, 40, 80, 160 μg/ml) for 72h. After treatment, cell viability was assessed with the use of CCK-8 (Dojindo, Japan); the expression of miR-146a as well as the mRNA expressions of IRAK1 and TRAF6 were determined by RT-qPCR, and the protein expressions of IRAK1, TRAF6, JNK1, and p-JNK1 were detected by western blot.

T614 treatment for plasmid-transfected RA-FLS

After transfection, the cells were divided into four groups and treated with or without T614 as follows:

1. Inhibitor-NC: the inhibitor-NC cells were incubated in the medium without T614;
2. Inhibitor-miR-146a: the inhibitor-miR-146a cells were incubated in the medium without T614;
3. T614&Inhibitor-NC: the inhibitor-NC cells were incubated in the medium with 20 μg/ml T614;
4. T614&Inhibitor-miR-146a: the inhibitor-miR-146a cells were incubated in the medium with 20 μg/ml T614.

Then the subsequent detections including cell proliferation, apoptosis, migration ability, invasion ability and the levels of TNF-α, IL-1, IL-6 and IL-17 in cell supernatant were performed as the method mentioned in "*Transfection and subsequent detection*" subsection. Moreover, the expressions of miR-146a, IRAK1, TRAF6, JNK1 and p-JNK1 were evaluated as the method mentioned in "*Assessment of pathway regulated by miR-146a*" subsection as well.

CIA model

Wistar rats with the age of 8–12 weeks old and the weight of 180±20 g were purchased from Shanghai Institutes for Biological Sciences (Shanghai, China). The rats were housed under specific pathogen-free conditions of 12h light/dark cycle with relative humidity of 55–65% at 22–26°C. All animal experiments were approved by Institutional Animal Care and Use Committee of our Hospital and conducted in accordance with the National Institutes of Health guidelines for the care and use of laboratory animals. CIA rats were established according to the method described previously (24). Briefly, the chicken type II collagen (Chondrex, USA) (4 mg/ml) and the complete Freund's adjuvant (Sigma, USA) were mixed in 1:1 volume ratio then injected to the tail root of the rats (the day of the first injection was recorded as day 0); on day 7, the chicken type II collagen (Chondrex, USA) (4 mg/ml) mixing with the incomplete Freund's adjuvant (Sigma, USA) in 1:1 volume ratio was injected to the tail root of the rats. On day 21 after first injection, CIA rats were divided into following groups: (1) model group (n=6), which was

given physiological saline (1 ml) by gavage and physiological saline (200 μl) through tail intravenous injection every other day for another 30 days; (2) Inhibitor-miR-146a group (n=6), which was given physiological saline (1 ml) by gavage and 250 μg (200 μl) miR-146a inhibitor plasmid through tail intravenous injection every other day for another 30 days; (3) T614 group (n=6), which was given T614 at dose of 20 mg/kg (1 ml) by gavage and physiological saline (200 μl) through tail intravenous injection every other day for 30 days; (4) T614&inhibitor-miR-146a group (n=6), which was given T614 at dose of 20 mg/kg by gavage and 250 μg (200 μl) miR-146a inhibitor plasmid through tail intravenous injection every other day for 30 days. Besides, the wistar rats (n=6) without any treatment were used as control group. During the intervention, the rats were observed every 3 days to assess the clinical presentations and the severity of arthritis, meanwhile the severity was evaluated according to a semi-quantitative clinical scoring system described previously (25). Details of the score system were as follows: 0, no arthritis; 1, definite erythema and swelling of the ankle or one digit; 2, two or more joints involved or mild erythema and swelling of the entire paw; 3, erythema and swelling extending from the ankle to the metatarsal joints of the entire paw and all digits; and 4, ankylosing deformity with severe joint erythema and swelling. The arthritis score for each rat was the sum of the scores of all paws with the maximum score being 16. On day 51, the rats were sacrificed, then the synovium of left hind paw isolated, which was divided into two parts, one was fixed with 10% formalin and paraffin-embedded, the other was properly stored at -80°C for subsequent detections. For the observation of pathologic morphology, the haematoxylin-eosin (H&E) staining was performed; for the evaluation of cell apoptosis, the Terminal-deoxynucleoitidyl Transferase Mediated Nick End Labeling (TUNEL) staining was carried out; for the assessment of protein expressions of TNF-α, IL-1β, IL-6, IL-17, IRAK1, TRAF6 and p-JNK1, the immunohistochemistry (IHC) staining was conducted. As for the detections of expressions of TNF-α, IL-1β, IL-6, IL-17, miR-146a, IRAK1 and TRAF6, the RT-qPCR was performed.

Table I. Primers sequences.

Gene	Forward Primer (5'-3')	Reverse Primer (5'-3')
Human		
IRAK1	TGTGGACACGGACACCTTCA	AGCCTCCTCAGCCTCCTCTT
TRAF6	ATGCCAGCGTCCCTTCCAA	GCGTGCCAAGTGATTCCTCT
GAPDH	GACCACAGTCCATGCCATCAC	ACGCCTGCTTCACCACCTT
miR-146a	ACACTCCAGCTGGGTGAGAACTGAATTCCA	TGTCGTGGAGTCGGCAATTC
U6	CGCTTCGGCAGCACATATACTA	ATGGAACGCTTCACGAATTTGC
Rat		
IRAK1	GCTCCTCCAGGTTCCACTCT	GCCTCCTCCTTCAGTCTCTTCA
TRAF6	GCGTCCAGCCAGTCTTCAAG	CCCGTAAAGCCATCAAGCAGAT
TNF-α	CGAGATGTGGAACTGGCAGAG	CACGAGCAGGAATGAGAAGAGG
IL-1β	GGACAGAACATAAGCCAACAAGTG	GTGGGTGTGCCGTCTTTCAT
IL-6	GGAGAGGAGACTTCACAGAGGA	ACTCCAGAAGACCAGAGCAGAT
IL-17	GCCTGATGCTGTTGCTGCTA	TGGAACGGTTGAGGTAGTCTGA
GAPDH	CAAGTTCAACGGCACAGTCAAG	ACATACTCAGCACCAGCATCAC
miR-146a	ACACTCCAGCTGGGTGAGAACTGAATTCCA	TGTCGTGGAGTCGGCAATTC
U6	CGCTTCGGCAGCACATATACTA	ATGGAACGCTTCACGAATTTGC

Table II. Antibody information of western bot

Antibody	Company	Dilution
Primary antibody		
Rabbit monoclonal to IRAK-1	Abcam (UK)	1:1000
Rabbit monoclonal to TRAF6	Abcam (UK)	1:5000
Mouse monoclonal to JNK1	Santa Cruz (USA)	1:1000
Rabbit monoclonal to JNK1 (phospho T183)	Abcam (UK)	1:1000
Rabbit monoclonal to GAPDH	CST (USA)	1:1000
Secondary antibody		
Goat anti-mouse IgG-HRP	Santa Cruz (USA)	1:5000
Goat anti-rabbit IgG H&L (HRP)	Abcam (USA)	1:10000

Table III. Antibody information of IHC staining.

Antibody	Company	Dilution
Primary antibody		
Rabbit monoclonal to IRAK-1	Abcam (UK)	1:250
Rabbit monoclonal to TRAF6	Abcam (UK)	1:50
Rabbit monoclonal to JNK1 (phospho T183)	Abcam (UK)	1:100
Mouse monoclonal to TNF alpha	Abcam (UK)	1:50
Rabbit polyclonal to IL-1 beta	Abcam (UK)	1:100
Rabbit polyclonal to IL-6	Abcam (UK)	1:500
Rabbit polyclonal to IL-17A	Invitrogen (USA)	1:100
Secondary antibody		
Goat anti-mouse IgG-HRP	Santa Cruz (USA)	1:200
Goat anti-rabbit IgG H&L (HRP)	Abcam (USA)	1:1000

RT-qPCR

Total RNA was extracted from cells or tissues with the use of TRIzol Reagent (Invitrogen, USA) following the kit instructions. After the assessment of integrity and quantity, the RNA was reversely transcribed to cDNA by KOD SYBR® qPCR Mix (Toyobo, Japan). Then, THUNDERBIRD® SYBR® qPCR Mix (Toyobo, Japan) was applied to perform the qPCR. U6 was set as the internal reference for miR-146a, and glyceraldehyde-phosphate dehydrogenase (GAPDH) was served as the internal reference for mRNAs. The primers in RT-qPCR were presented in Table I.

Western blot

The protein was extracted from cells or tissues using RIPA Lysis Buffer (Thermo, USA), which was quantified by Bicinchoninic Acid Kit for Protein Determination (Sigma, USA). Then

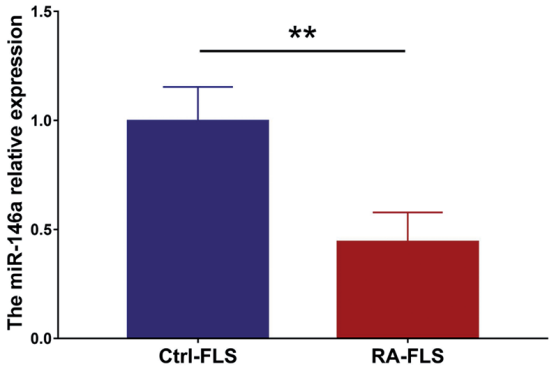

Fig. 1. The miR-146a expression in Ctrl-FLS and RA-FLS.
MiR: microRNA; RA-FLS: rheumatoid arthritis-fibroblast-like synoviocytes; Ctrl-FLS: control-fibroblast-like synoviocytes

the electrophoresis of the extracted protein was performed using 8%-12% SDS-PAGE Gels (Thermo, USA), after which the protein was transferred to a nitrocellulose filter membrane (PALL, USA). Subsequently, the membrane was blocked with bovine serum albumin (BSA) (Sigma, USA) and incubated with primary antibody at 4°C overnight, which was then incubated with secondary antibody at room temperature for 2 h. Afterward, chemiluminescence was carried out using the Pierce® ECL Plus Western Blotting Substrate (Invitrogen, USA), and the results were exposed using x-ray film (Fuji film, Japan) and viewed on Gel Imager (Thermo, USA) as x-ray film (Fuji film, Japan). Antibodies were presented in the Table II.

Scratch wound healing assay

Initially, the cells were seeded in a 24-well plate for preparation. One day after the seed, each well on the plate was scratched using a 10 µl tip. Then the scratched lines in each well were taken a picture using the BX41 microscope (Olympus, Japan) at 0 hr and 24 hr post scratching.

Transwell assay

200 µl single cell suspension that consisted of 1% FBS was added into the upper side of transwell chamber coated with Matrigel® Basement Membrane Matrix (BD, USA), then 500 µl culture medium containing 10% FBS was added into the lower side of transwell chamber. Subsequently, the cells were put into an incubator for 24 hr. After which, the transwell chamber was fixed with 4% formaldehyde (Sigma, USA) after the non-invasive cells were wiped off, which lasted for 30 mins, and washed with PBS for three times. And 0.1% crystal violet (Sigma, USA) was used to dye the cells at room temperature for 20 mins. Finally, the pictures

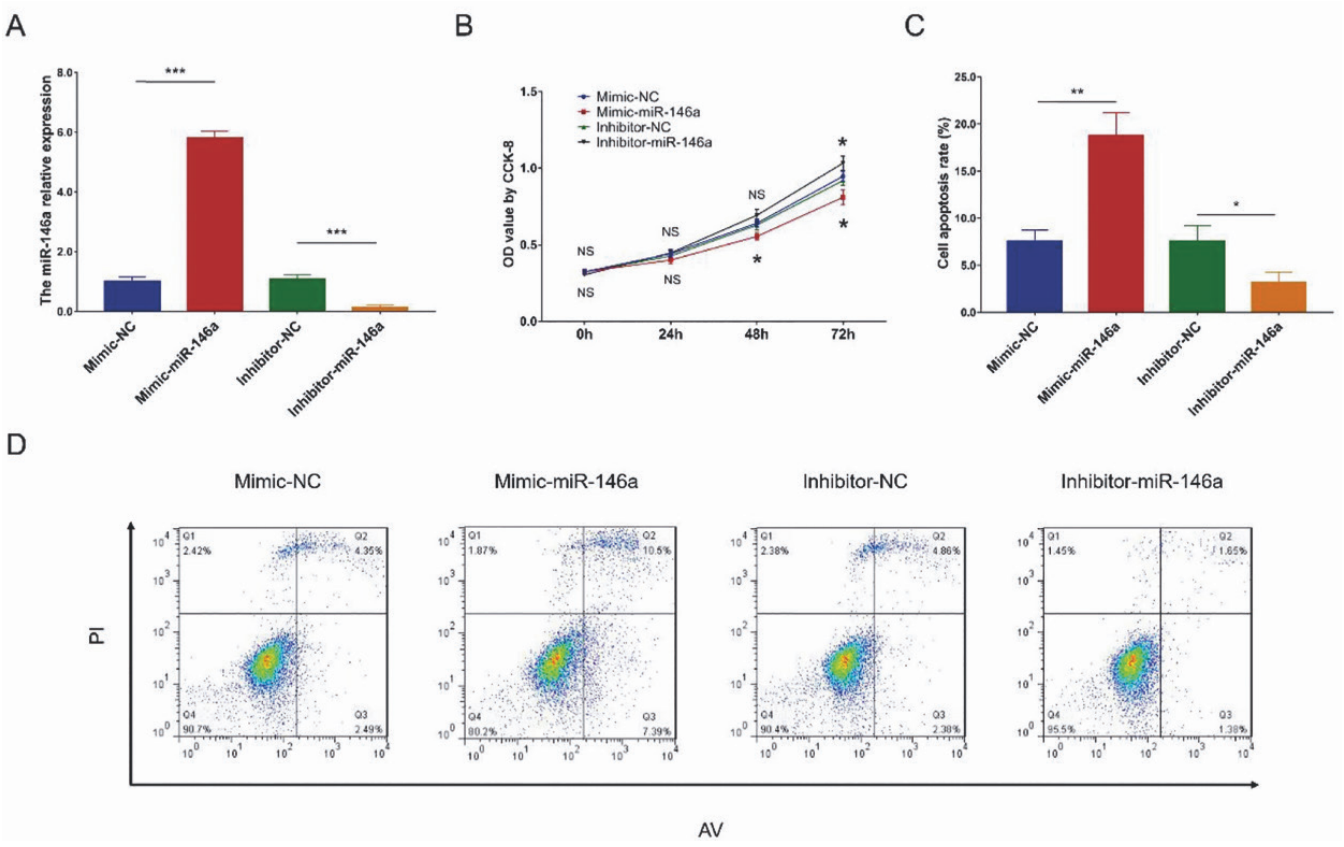

Fig. 2. The effect of miR-146a on proliferation and apoptosis of RA-FLS. MiR-146a relative expression after transfection (**A**), comparison of OD value by CCK-8 between groups (**B**), and comparison of cell apoptosis rate between groups (**C**-**D**).
MiR: microRNA; RA-FLS: rheumatoid arthritis-fibroblast-like synoviocytes; OD: optical density; CCK-8: cell counting kit-8; NC: negative control; PI: Propidium Iodide; AV: Annexin V.

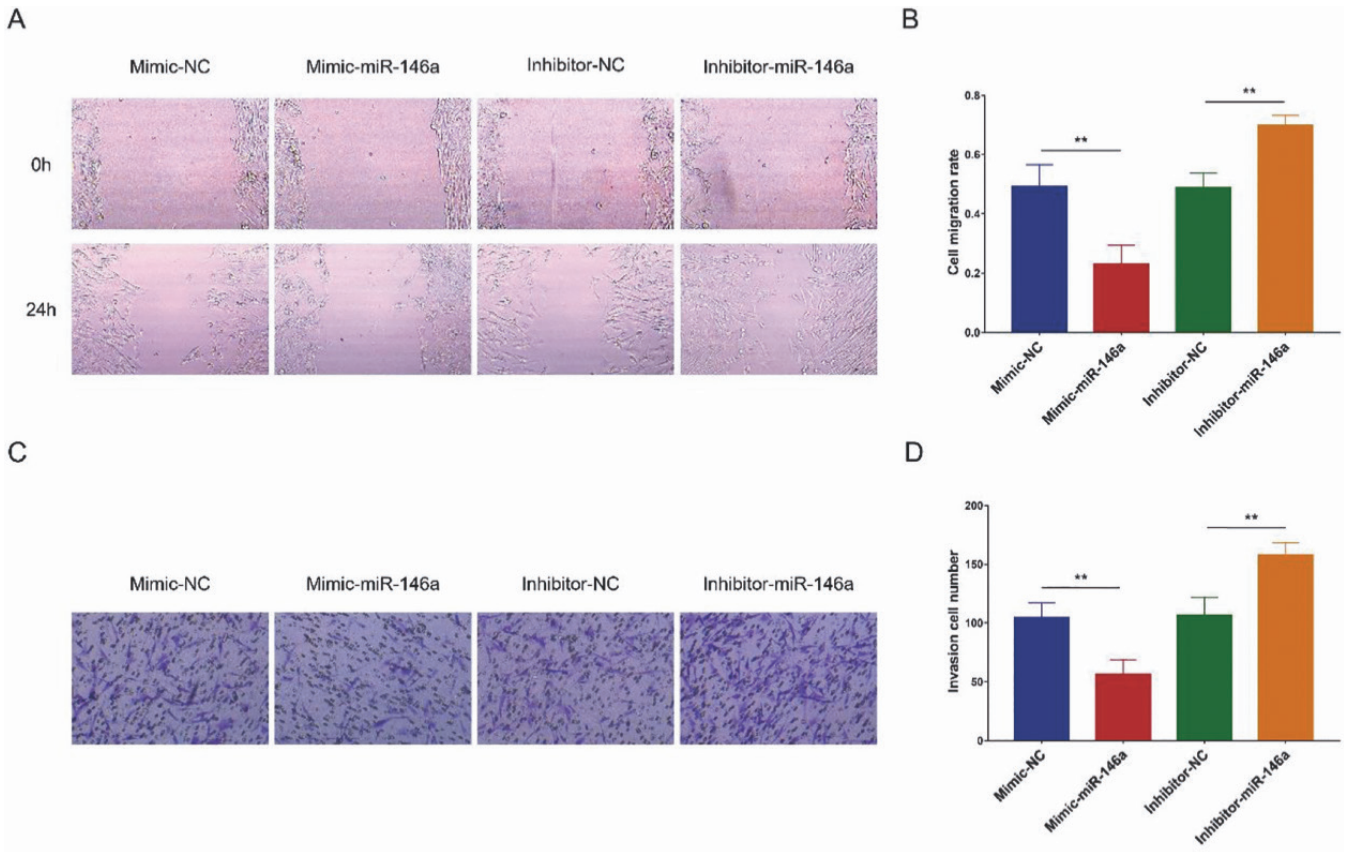

Fig. 3. The effect of miR-146a on migration and invasion of RA-FLS. The examples of scratch wound healing assay pictures (**A**), comparison of cell migration rate between groups (**B**), the examples of transwell assay pictures (**C**), comparison of invasive cell number between groups (**D**).
MiR: microRNA; RA-FLS: rheumatoid arthritis-fibroblast-like synoviocytes; NC: negative control,

were taken using a BX41 microscope (Olympus, Japan), and the number of invasive cells was counted.

H&E, TUNEL and IHC staining

HE staining was performed with the use of Haematoxylin and Eosin Staining Kit (Beyotime, China) in accordance with the standard protocol of the kit. TUNEL staining was completed by the One Step TUNEL Apoptosis Assay Kit (Beyotime, China) in terms of the manufacturer's protocol. The number of TUNEL positive cells was calculated in five selected fields. The TUNEL positive cell rates were calculated through the number of TUNEL positive cells divided by the number of total cells. IHC assay was done following the standard operating protocol of the Early Detection Research Network (EDRN). The antibodies for IHC were listed in Table III.

Statistical analysis

The data in this study were expressed as mean and standard deviation (SD). Statistical analyses and graph plotting were performed on GraphPad Prism 7.01 (GraphPad Software, USA). Comparison between two independent groups was determined by the unpaired t-test. The multiple comparisons in this study were all comparisons between a control group and other experiment groups, therefore, these multiple comparisons were determined by the one-way ANOVA test followed by Dunnett-t test. p-value <0.05 indicated statistically significant. Furthermore, p-value <0.05, <0.01, and <0.001 were respectively displayed as "*", "**", and "***", while p-value >0.05 (not significant) was displayed as "NS" in the figures.

Results

MiR-146a regulated proliferation, apoptosis, migration and invasion of RA-FLS

MiR-146a was downregulated in RA-FLS compared to Ctrl-FLS (p<0.01) (Fig. 1). Post transfection in RA-FLS, miR-146a was increased in the mimic-miR-146a group compared to the mimic-NC group (p<0.001) (Fig. 2A), but was reduced in the inhibitor-miR-146a group than that of the inhibitor-NC group. The cell proliferation was reduced in the mimic-miR-146a group compared to the mimic-NC group, while it was elevated in the inhibitor-miR-146a group compared to the inhibitor-NC group (p<0.05) (Fig. 2B). The cell apoptosis rate was increased in the mimic-miR-146a group compared to the mimic-NC group (p<0.01), however, it was decreased in the inhibitor-miR-146a group compared to the inhibitor-NC group (p<0.05) (Fig. 2C-D). As for the cell migration (Fig. 3A-B) and invasion (Fig. 3C-D), they were reduced in the mimic-miR-146a group compared with the mimic-NC group, while they were promoted in the inhibitor-miR-146a group compared to the inhibitor-NC group (all p<0.01).

MiR-146a reduced pro-inflammatory cytokines in RA-FLS

In terms of pro-inflammatory cytokines, the levels of TNF-α (Fig. 4A),

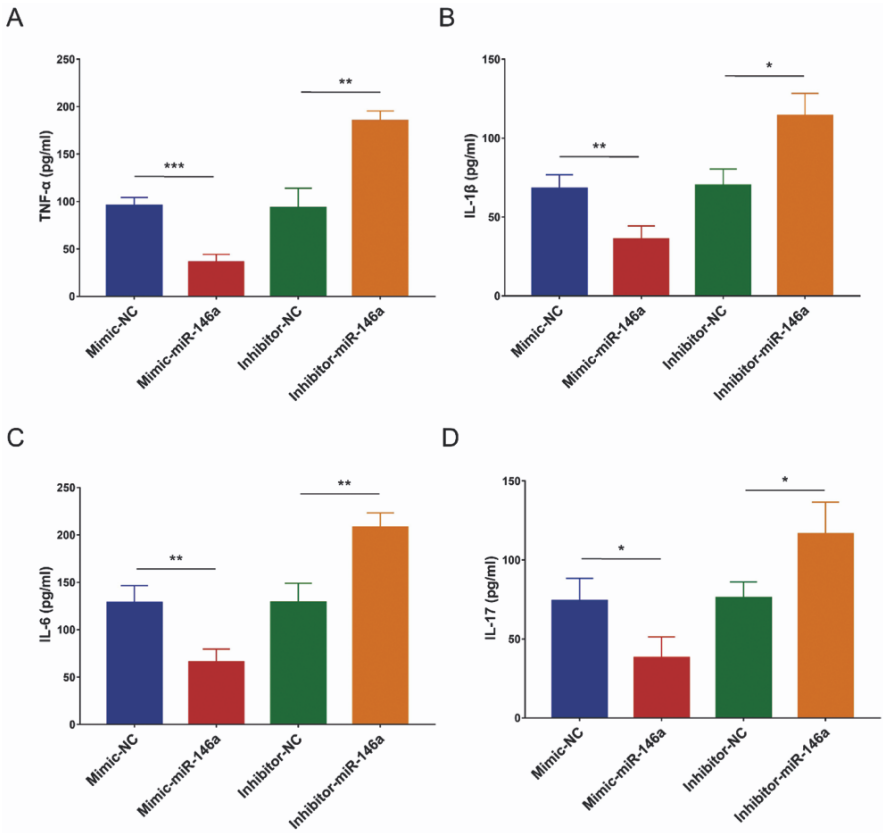

Fig. 4. The effect of miR-146a on pro-inflammatory cytokines in RA-FLS. Comparison of supernatant TNF-α (**A**), IL-1β (**B**), IL-6 (**C**) and IL-17 (**D**) mRNA expressions between groups.
MiR: microRNA; RA-FLS: rheumatoid arthritis-fibroblast-like synoviocytes; TNF-α, tumour necrosis factor-α; IL: interleukin; NC: negative control.

IL-1β (Fig. 4B), IL-6 (Fig. 4C) and IL-17 (Fig. 4D) in cell supernatant of RA-FLS were all inhibited in Mimic-miR-146a group compared to Mimic-NC group, while were enhanced in Inhibitor-miR-146a group than those in Inhibitor-NC group (all $p<0.05$).

MiR-146a suppressed IRAK1 and TRAF6/JNK1 pathway in RA-FLS

The IRAK1 mRNA was downregulated in the mimic-miR-146a group than that in the mimic-NC group ($p<0.05$), while it was upregulated in the inhibitor-miR-146a group compared to the inhibitor-NC group ($p<0.01$) (Fig. 5A). In addition, the TRAF6 mRNA was also decreased in the mimic-miR-146a group compared to the mimic-NC group ($p<0.01$), while it was increased in the inhibitor-miR-146a group than that in the inhibitor-NC group ($p<0.01$) (Fig. 5B). In terms of the proteins, the IRAK1, TRAF6 and p-JNK1 protein expressions were diminished in the mimic-miR-146a group compared to the mimic-NC group while they were elevated in the inhibitor-miR-146a group compared to the inhibitor-NC group (Fig. 5C).

Iguratimod regulated cell viability, miR-146a, IRAK1 and TRAF6/JNK1 pathway in RA-FLS

Post-iguratimod treatment in RA-FLS, the cell viability was decreased at the concentrations of 20 μg/ml, 40 μg/ml, 80 μg/ml and 160 μg/ml iguratimod than that with no iguratimod treatment (all $p<0.001$) (Fig. 6A). Additionally, miR-146a (Fig. 6B) was increased while the IRAK1 mRNA (Fig. 6C) and TRAF6 mRNA (Fig. 6D) were decreased in RA-FLS treated with 20 μg/ml, 40 μg/ml, 80 μg/ml and 160 μg/ml iguratimod compared to no iguratimod treatment (all $p<0.05$). The above-mentioned changes indicated that miR-146a, IRAK1 mRNA, and TRAF6 mRNA were decreased in a dose-dependent manner in iguratimod treated RA-FLS. Besides, IRAK1, TRAF6 and p-JNK1 proteins were also decreased

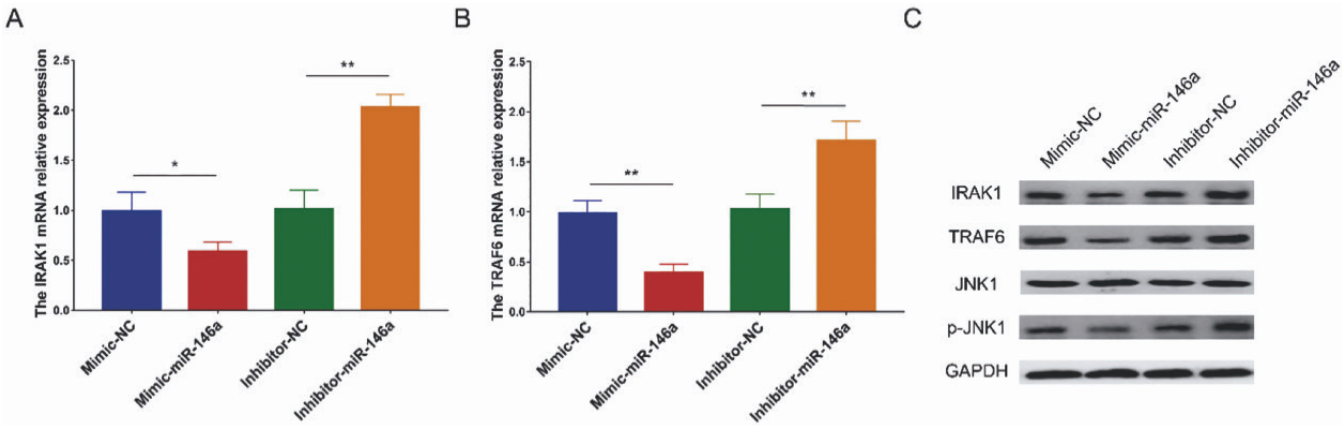

Fig. 5. The effect of miR-146a on IRAK1 and TRAF6/JNK1 pathway in RA-FLS.
Comparison of IRAK1 mRNA relative expression (**A**), TRAF6 mRNA relative expression (**B**), and protein expressions of IRAK1, TRAF6, JNK1, p-JNK1 (**C**) bewteen groups.
MiR: microRNA; IRAK1: interleukin 1 receptor associated kinase 1; TRAF6: TNF receptor associated factor 6; JNK1: c-Jun NH2-terminal kinase 1; RA-FLS: rheumatoid arthritis-fibroblast-like synoviocytes; p-JNK1: phosphorylated-JNK1; NC: negative control.

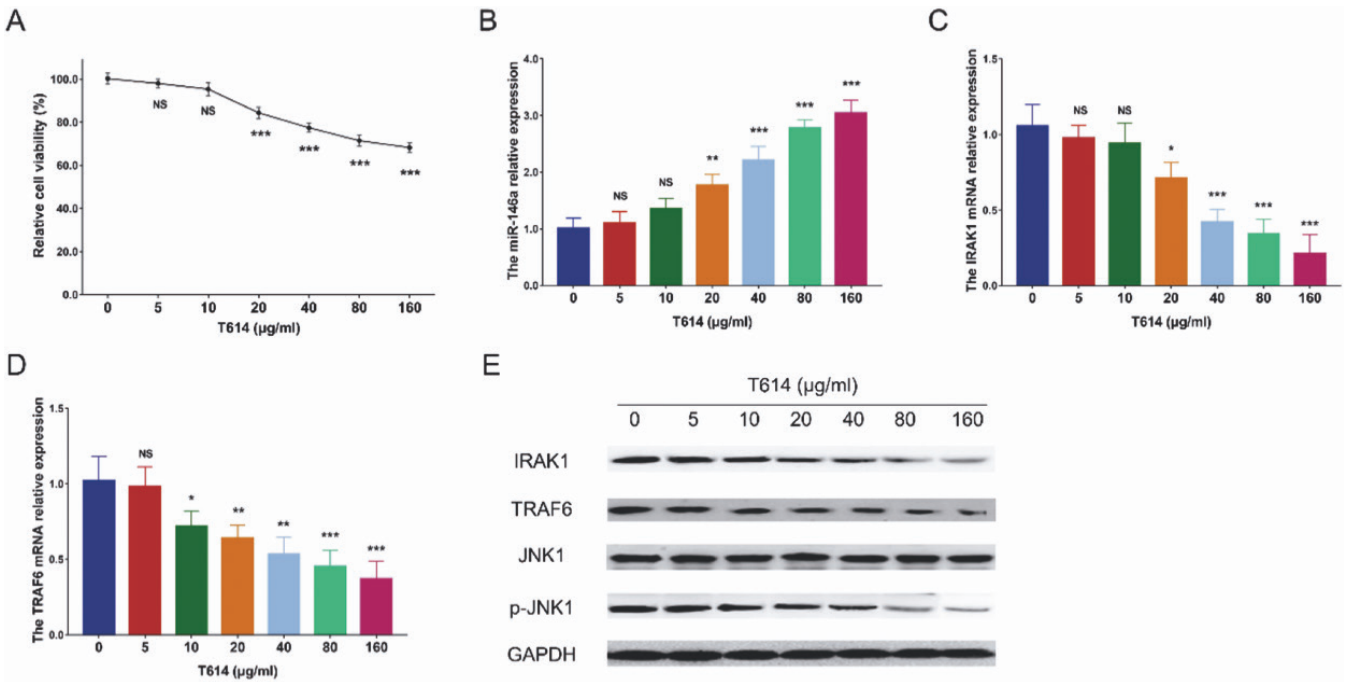

Fig. 6. The effect iguratimod on cell viability, miR-146a, IRAK1 and TRAF6/JNK1 pathway in RA-FLS. Relative cell viability (**A**), miR-146a relative expression (**B**), IRAK1 mRNA relative expression (**C**), TRAF6 mRNA relative expression (**D**), and IRAK1, TRAF6, JNK1, p-JNK1 protein expressions (**E**) in RA-FLS treated with different doses of Iguratimod.
MiR: microRNA; IRAK1: interleukin 1 receptor associated kinase 1; TRAF6: TNF receptor associated factor 6; JNK1: c-Jun NH2-terminal kinase 1; RA-FLS: rheumatoid arthritis-fibroblast-like synoviocytes; p-JNK1: phosphorylated-JNK1; GAPDH: glyceraldehyde-phosphate dehydrogenase.

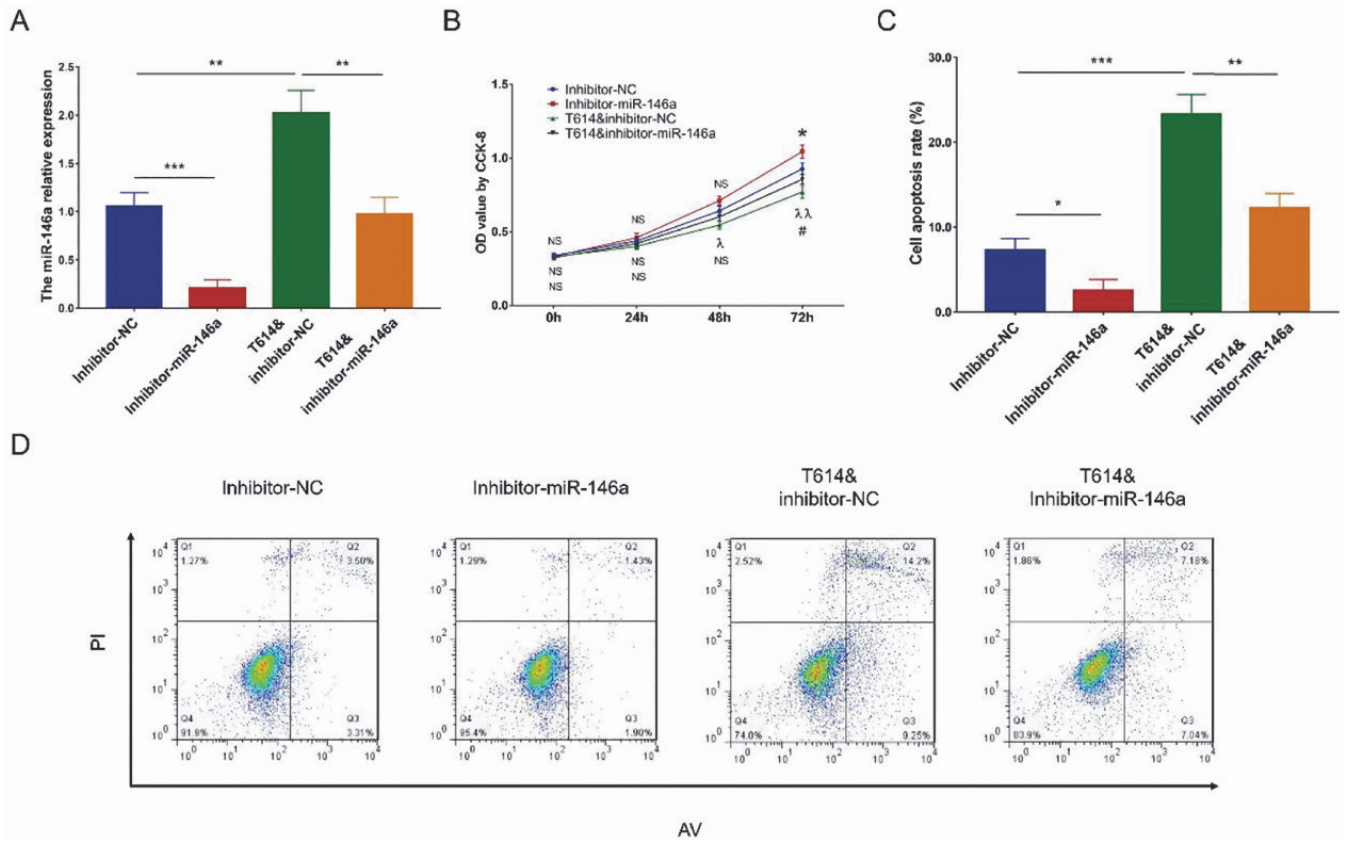

Fig. 7. MiR-146a inhibition mediated the effect of iguratimod on proliferation and apoptosis of RA-FLS. Comparisons of miR-146a relative expression (**A**), OD value by CCk-8 (**B**), cell apoptosis rate (**C**-**D**) between groups post transfection.
MiR: microRNA; RA-FLS: rheumatoid arthritis-fibroblast-like synoviocytes; OD: optical density; NC: negative control; CCK-8: cell counting kit-8.

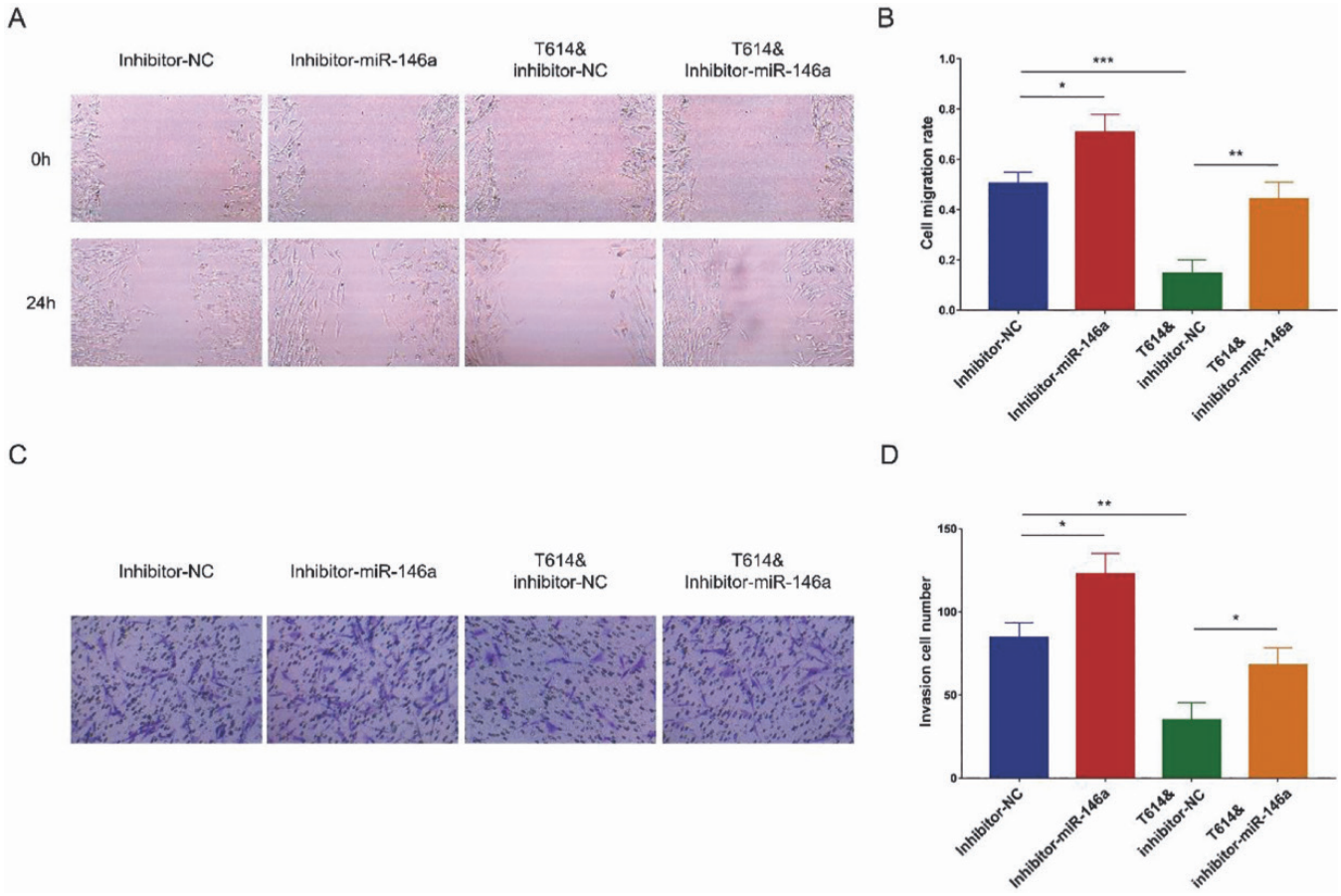

Fig. 8. MiR-146a inhibition regulated the effect of iguratimod on migration and invasion of RA-FLS. Examples of wound healing assay pictures (**A**), comparison of cell migration rate between groups (**B**), examples of transwell assay pictures (**C**), comparison of invasive cell number (**D**) between groups. MiR: microRNA; RA-FLS: rheumatoid arthritis-fibroblast-like synoviocytes; NC: negative control.

in a dose-dependent manner in iguratimod treated RA-FLS (Fig. 6E).

MiR-146a inhibition attenuated the effect of iguratimod on regulating cell functions of RA-FLS

After the transfection, miR-146a was elevated in the T614&inhibitor-NC group compared with the inhibitor-NC group ($p<0.01$), while it was decreased in the T614&inhibitor-miR-146a group than that in the T614&inhibitor-NC group ($p<0.01$) (Fig. 7A). The cell proliferation post transfection was decreased in the T614&inhibitor-NC group compared to the inhibitor-NC group; however, it was elevated in the T614&inhibitor-miR-146a group compared to the T614&inhibitor-NC group (all $p<0.01$) (Fig. 7B). As for cell apoptosis rate, it was higher in the T614&inhibitor-NC group compared to the inhibitor-NC group, but was lower in the T614&inhibitor-miR-146a group compared with the T614&inhibitor-NC group ($p<0.01$) (Fig. 7C-D). In terms of cell migration (Fig. 8A-B) and invasion (Fig. 8C-D), they were both decreased in the T614&inhibitor-NC group compared to the inhibitor-NC group, but were increased in the T614&inhibitor-miR-146a group compared to the T614&inhibitor-NC group (all $p<0.05$). These results implied that iguratimod suppressed cell proliferation, migration and invasion while it enhanced apoptosis of RA-FLS by upregulating miR-146a.

MiR-146a inhibition diminished the effect of iguratimod on regulating inflammation in RA-FLS

The TNF-α (Fig. 9A), IL-1β (Fig. 9B), IL-6 (Fig. 9C) and IL-17 (Fig. 9D) levels in cell supernatant of RA-FLS were all reduced in the T614&inhibitor-NC group compared with the inhibitor-NC group, while they were increased in the T614&inhibitor-miR-146a group compared to the T614&inhibitor-NC group (all $p<0.05$). These data indicated that iguratimod repressed inflammation via upregulating miR-146a in RA-FLS.

MiR-146a inhibition suppressed the effect of iguratimod on regulating IRAK1 and TRAF6/JNK1 pathway in RA-FLS

The IRAK1 (Fig. 10A) and TRAF6 (Fig. 10B) mRNAs were repressed in the T614&inhibitor-NC group compared to the inhibitor-NC group, but were promoted in the T614&inhibitor-miR-146a group compared with the T614&inhibitor-NC group (all $p<0.05$). The IRAK1, TRAF6 and JNK1 proteins were decreased in the T614&inhibitor-NC group than those in the inhibitor-NC group, while they were elevated in the T614&inhibitor-miR-146a group compared with the T614&inhibitor-NC group (Fig. 10C). These results suggested that iguratimod downregulated IRAK1 and TRAF6/JNK1 pathway via upregulating miR-146a in RA-FLS.

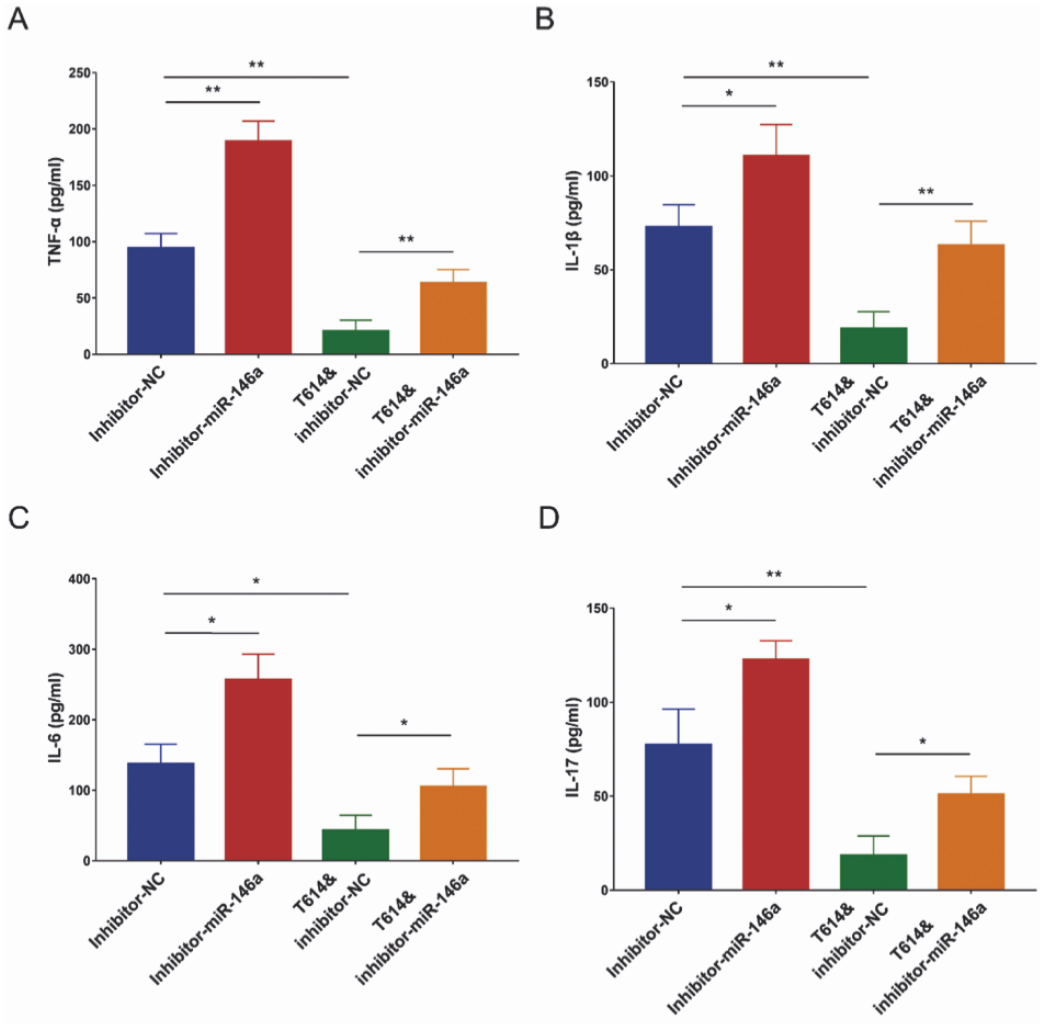

Fig. 9. MiR-146a inhibition modulated the effect of iguratimod on pro-inflammatory cytokines in RA-FLS. The comparisons of supernatant TNF-α (**A**), IL-1β (**B**), IL-6 (**C**) and IL-17 (**D**) mRNA relative expressions between groups.
MiR: microRNA;
RA-FLS: rheumatoid arthritis-fibroblast-like synoviocytes;
TNF-α: tumour necrosis factor-α;
ùIL: interleukin;
NC: negative control.

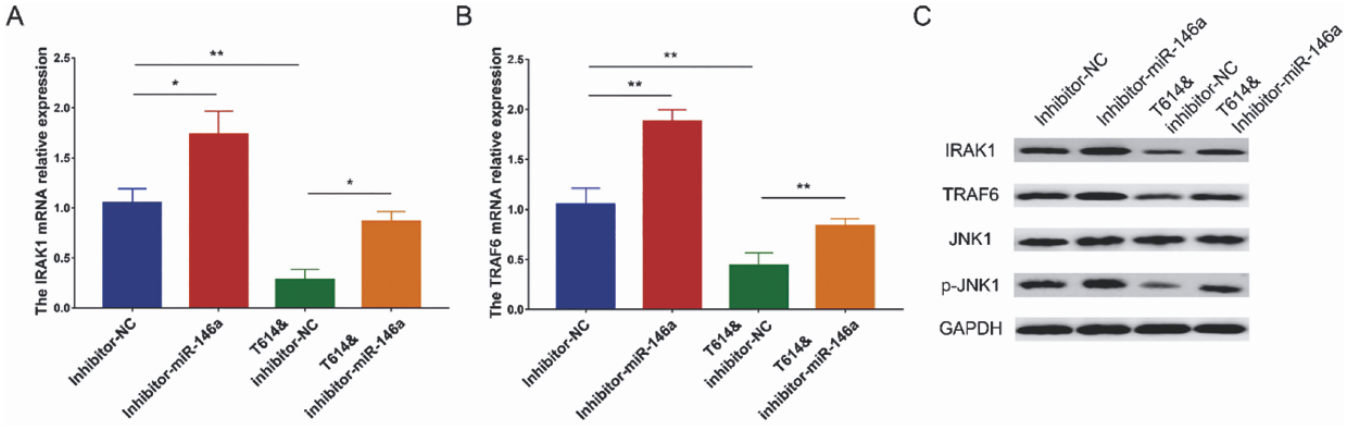

Fig. 10. MiR-146a inhibition regulated the effect of iguratimod on IRAK1 and TRAF6/JNK1 pathway in RA-FLS. The comparison of IRAK1 mRNA relative expression (**A**), TRAF6 mRNAs relative expression (**B**), and IRAK1, TRAF6, JNK1, p-JNK1 protein expressions (**C**) between groups.
MiR, microRNA; IRAK1: interleukin 1 receptor associated kinase 1; TRAF6: TNF receptor associated factor 6; JNK1: c-Jun NH2-terminal kinase 1; RA-FLS: rheumatoid arthritis-fibroblast-like synoviocytes; p-JNK1: phosphorylated-JNK1; NC: negative control; GAPDH: glyceraldehyde-phosphate dehydrogenase.

Iguratimod was effective in treating CIA rat model via interacting with miR-146a

In CIA rat model, in terms of arthritis score, it was elevated in the inhibitor-miR-146a group compared to the model group and in the T614&inhibitor-miR-146a compared to the T614 group, while it was decreased in the T614 group compared to the model group at 33 d, 36 d, 39 d, 42 d, 48 d, and 51 d (all $p<0.05$) (Fig. 11A). As to histopathological features of synovial tissue assessed by HE staining, the hyperproliferation of synoviocytes and inflam-

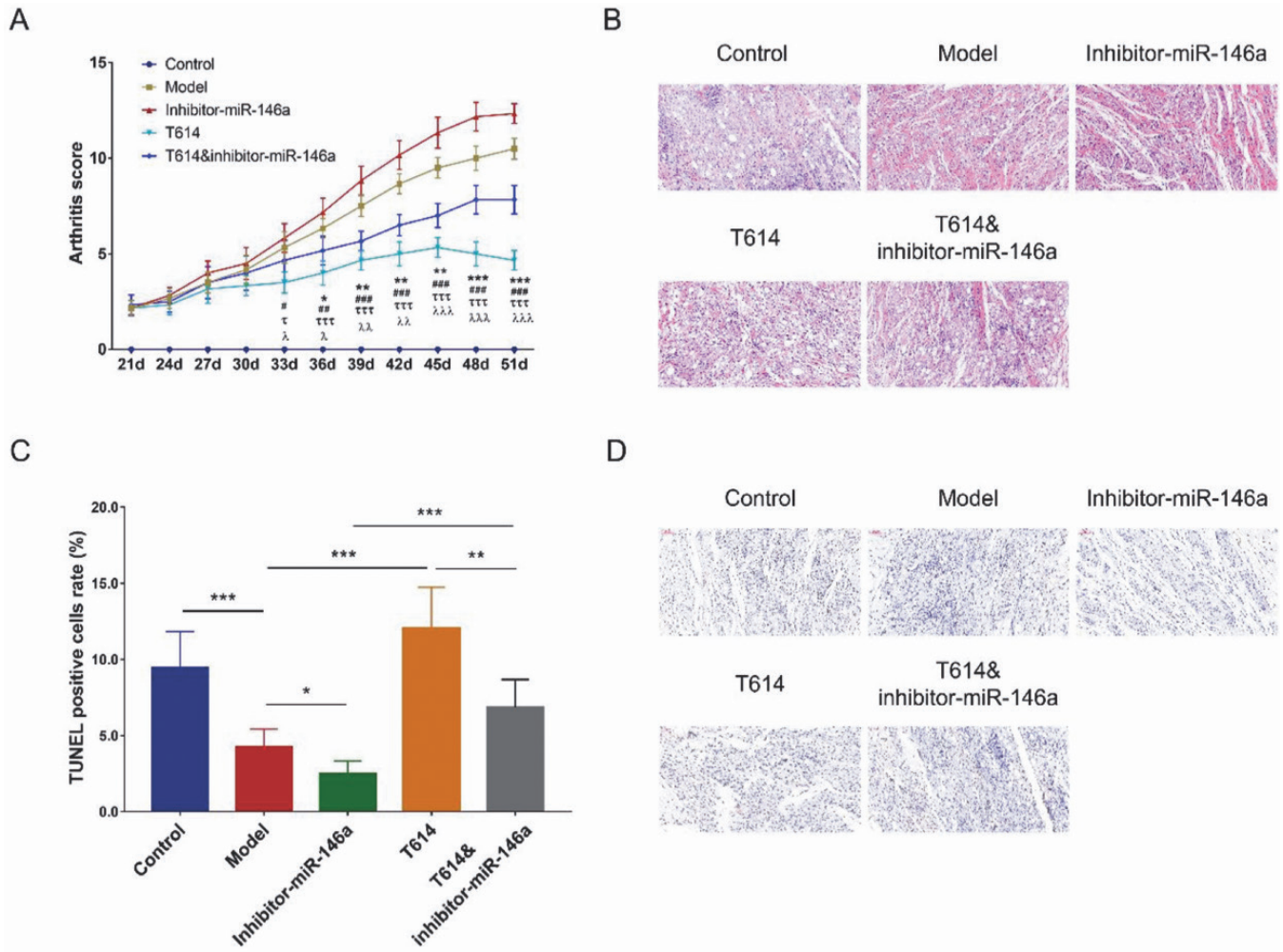

Fig. 11. Effect of miR-146a inhibition, iguratimod treatment and their combination on arthritis score and apoptosis in CIA rat model. Comparison of arthritis score between groups (**A**), examples of HE staining of synovial tissue (**B**), comparison of TUNEL positive cells rate in synovial tissue between groups (**C**), and examples of TUNEL staining of synovial tissue (**D**).
MiR: microRNA; CIA: collagen-induced arthritis; HE: haematoxylin-eosin; TUNEL: TdT-mediated dUTP Nick-End Labeling.

mation infiltration of synovial tissue were more severe in the inhibitor-miR-146a group compared to the model group and in the T614&inhibitor-miR-146a group compared with the T614 group, while they were relieved in the T614 group compared to the model group (Fig. 11B). As for the cell apoptosis of synovial tissue, the apoptosis rate (assessed by TUNEL assay) was decreased in the inhibitor-miR-146a group compared with the model group, and in the T614&inhibitor-miR-146a group compared with T614 group, however, it was elevated in the T614 group compared with the model group (all $p<0.05$) (Fig. 11C, D). With respect to the pro-inflammatory cytokines of synovial tissue, the mRNAs of TNF-α (Fig. 12A), IL-1β (Fig. 12B), IL-6 (Fig. 12C) and IL-17 (Fig. 12D) were all increased in the inhibitor-miR-146a group compared to the model group, and in T614&inhibitor-miR-146a group than those in the T614 group, whereas, they were downregulated in the T614 group compared to the model group (all $p<0.05$). In addition, the IHC staining revealed that the TNF-α, IL-1β, IL-6 and IL-17 proteins of synovial tissue showed similar trends as their mRNAs did between groups (Fig. 12E).

Iguratimod regulated miR-146a, IRAK1 and TRAF6/JNK1 pathway in CIA rat model

In synovial tissue collected from CIA rat model, miR-146a was downregulated in the inhibitor-miR-146a group compared to the model group and in the T614&inhibitor-miR-146a group than that in the T614 group, while it was upregulated in the T614 group compared to the model group (all $p<0.01$) (Fig. 13A). The IRAK1 mRNA (Fig. 13B) and TRAF6 mRNA (Fig. 13C) were increased in the inhibitor-miR-146a group compared with the model group, and in the T614&inhibitor-miR-146a group compared to the T614 group; nonetheless, they were decreased in the T614 group compared to the model group (all $p<0.05$). According to IHC staining, the IRAK1 and TRAF6 proteins of synovial tissue displayed the similar trends as the IRAK1 and TRAF6 mRNAs did between groups (Fig. 13D). As for p-JNK1 protein of synovial tissue, it was increased in the inhibitor-miR-146a group compared with the model group, and in the T614&inhibitor-miR-146a group compared to the T614 group; nevertheless,

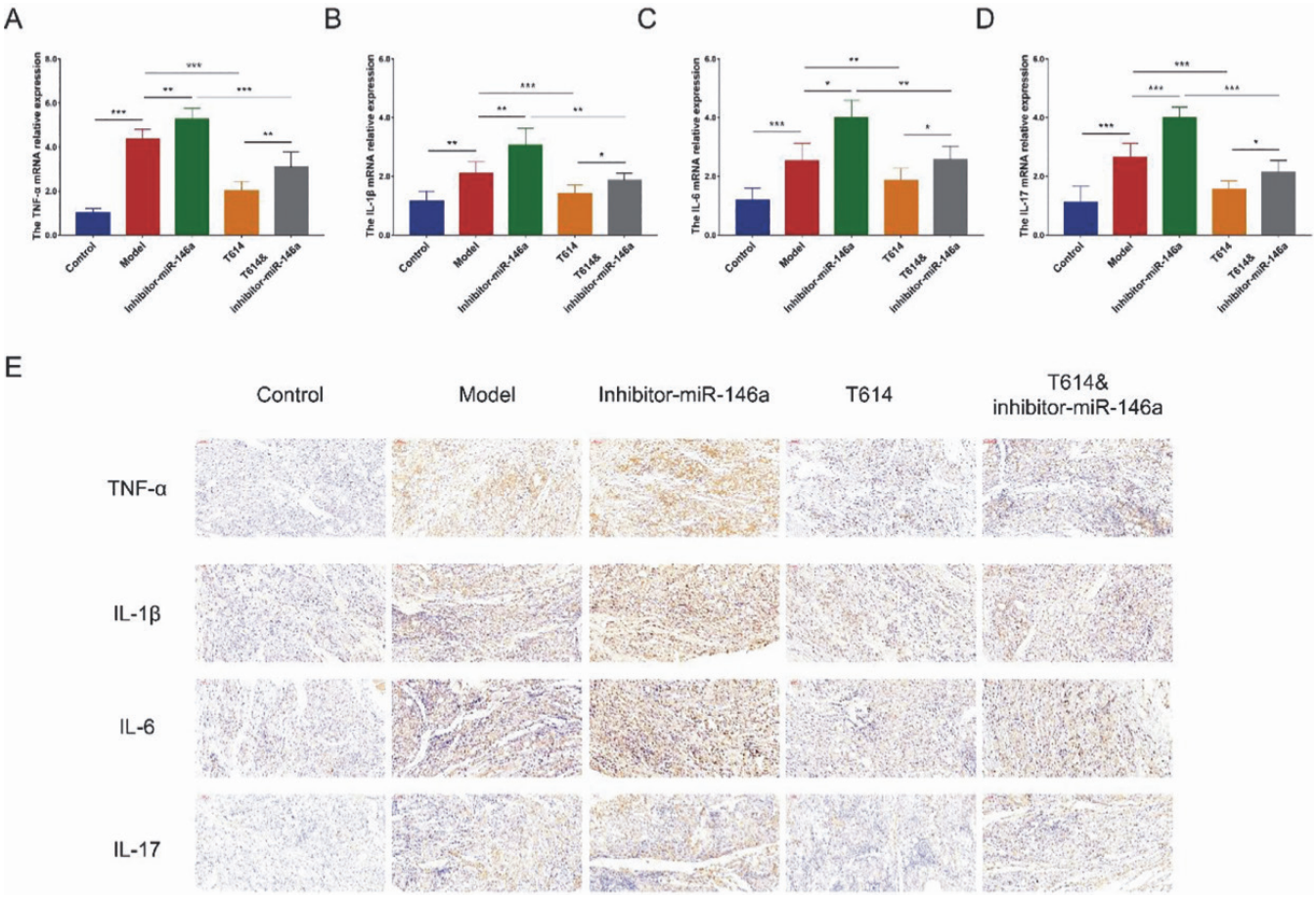

Fig. 12. Effect of miR-146a inhibition, iguratimod treatment and their combination on pro-inflammatory cytokines in CIA rat model. Comparison of TNF-α (**A**), IL-1β (**B**), IL-6 (**C**), IL-17 (**D**) mRNAs relative expressions, and their protein expressions (**E**) assessed by IHC staining in synovial tissue between groups. MiR: microRNA; CIA: collagen-induced arthritis; TNF-α: tumour necrosis factor-α; IL: interleukin; IHC: immunohistochemistry.

it was decreased in the T614 group compared to the model group.

Discussion

RA is a common inflammatory and autoimmune disease that predominantly damages the joints, thus, novel drugs for RA mostly target the factors related to systemic inflammation/immune dysregulation to relieve the injuries of synovial tissues in the joints (4, 26). Recent studies have revealed the critical roles of miRNAs in therapeutic effect of drug treatment in RA patients, for instance, an increase of miR-10a expression is observed in RA patients who are treated with methotrexate (27). Moreover, although iguratimod is one of the most promising drugs in treating RA, no effort has been made to explore the role of miRNA in the therapeutic effect of iguratimod in RA. Since iguratimod had been reported to ameliorate RA by acting as a MIF inhibitor, and miR-146a could modulate MIF expression, we evaluated the regulatory effect of iguratimod on miR-146a and its downstream gene/pathway in treating RA *in vivo* and *in vitro* (18). The results of our study showed that: (1) miR-146a inhibited cell proliferation, invasion, migration, inflammation, IRAK1, and TRAF6/JNK1 pathway while promoted the apoptosis in RA-FLS; (2) iguratimod reduced cell viability, miR-146a, IRAK1 and TRAF6/JNK1 pathway in a dose-dependent manner, and it repressed cell proliferation, migration, invasion, inflammation while promoted apoptosis by modulating miR-146a and its downstream gene IRAK1 as well as its downstream pathway TRAF6/JNK1 in RA-FLS; (3) Iguratimod reduced the arthritis score of CIA rat, and enhanced cell apoptosis while reduced inflammation in synovial tissue from CIA rat through regulating miR-146a and its downstream gene IRAK1 as well as downstream pathway TRAF6/JNK1.

MiR-146a is one of the most crucial miRNAs participating in both innate and adaptive immunity as well as inflammation (28). To be exact, a previous study reveals that miR-146a inhibition promotes the production of IL-6 that results in more severe inflammation in lipopolysaccharide-stimulated cystic fibrosis macrophages (29). Besides, miR-146a reduces the inflammatory responses through targeting Toll-like receptor (TLR3) and TRAF6 in Coxsackievirus B virus infected cells (30). Another study reveals that miR-146a displays the protective effect against intracerebral haemorrhage via suppressing inflammation and oxidative stress in a rat model (31). In addition, a prior study elucidates that mice with miR-146a deficiency develop immune complex glomerulonephritis along with aging (32). The recognition of miR-146a

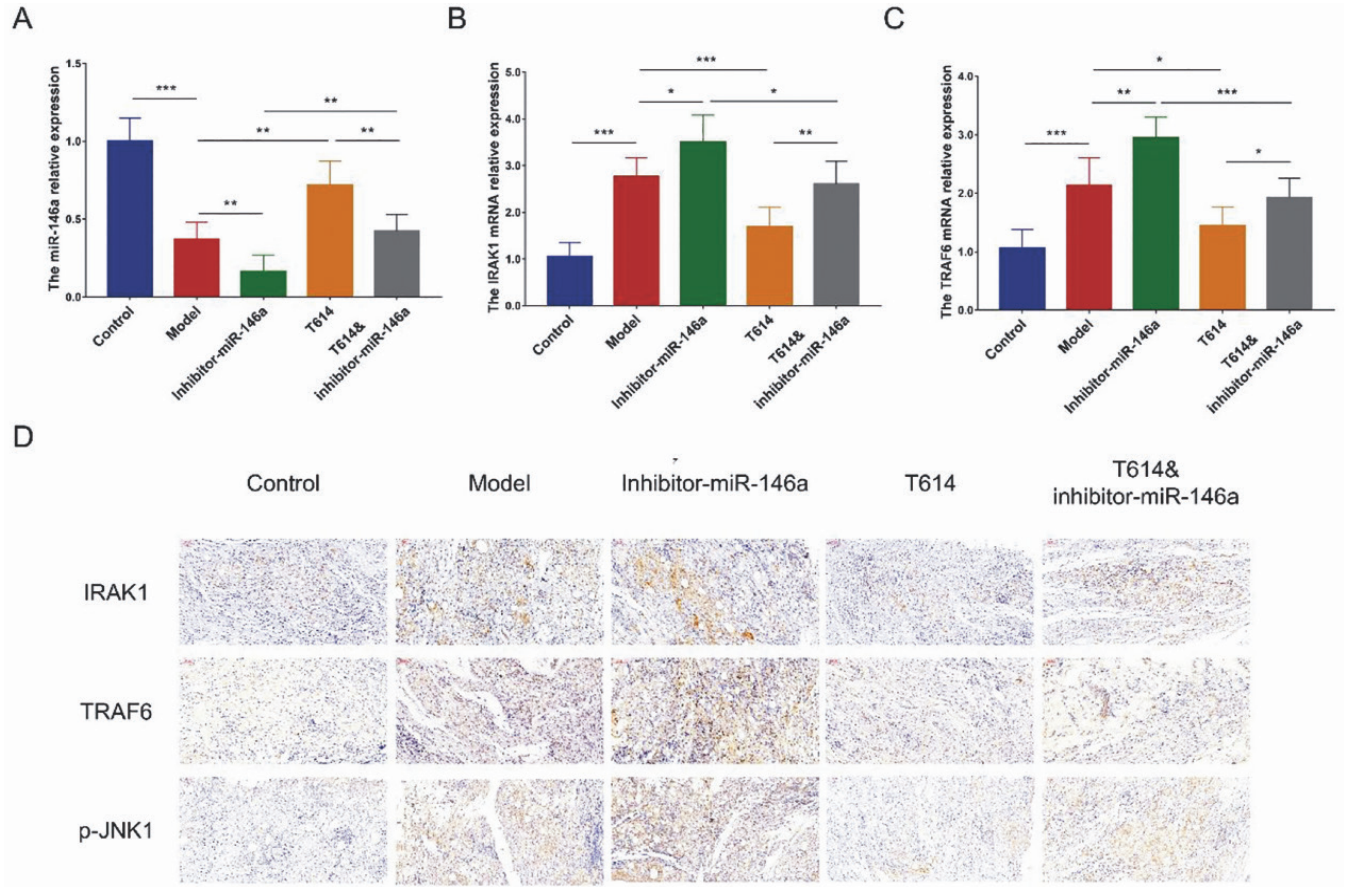

Fig. 13. Effect of miR-146a inhibition, iguratimod treatment and their combination on IRAK1 and TRAF6/JNK1 pathway in CIA rat model. Comparisons of miR-146a relative expression (**A**), IRAK1 mRNA relative expression (**B**), TRAF6 mRNA relative expression (**C**), and the protein expressions of IRAK1, TRAF6 as well as pJNK-1 (**D**) in synovial tissue between groups.
MiR: microRNA; IRAK1: interleukin 1 receptor associated kinase 1; TRAF6: TNF receptor associated factor 6; JNK1: c-Jun NH2-terminal kinase 1; CIA: collagen-induced arthritis; p-JNK1: phosphorylated-JNK1; IHC: immunohistochemistry.

wild-type 3' is required for a normal innate immune function in mice (33). These studies all indicate that miR-146a is an important regulator in reducing inflammation and balancing abnormal immune responses. In our study, miR-146a was found to repress cell proliferation, migration, invasion, inflammation, IRAK1, and TRAF6/JNK1 pathway while enhance cell apoptosis in RA-FLS, which could be explained by the following reasons: (1) miR-146a might play a protective role in RA via inhibiting cell proliferation, migration, invasion and inflammation while promoting cell apoptosis of RA-FLS through targeting multiple proteins, such as TLR3 and TRAF6, or reducing oxidative stress as found in other inflammation and immunity related diseases (28-33); (2) miR-146a might also regulate RA-FLS functions and inflammation by negatively mediating IRAK1 and TRAF6/JNK1 pathway as elucidated in our study. In addition, concerning that miR-146a is a risk factor for cardiac diseases and cardiac events, it could be speculated that elevation of miR-146a may increase the cardiac disease/event risk in RA patients. However, like many other miRNAs, miR-146a has a dual function in cardiac disease, such as, a previous study reveals that miR-146a reverses the cardiotoxicity caused by doxorubicin via reducing cardiomyocyte apoptosis and improving cardiomyocyte autophagy through mediating TATA-binding protein (TBP) associated factor 9b/P53 pathway (34). Besides, there is still no evidence elucidating that elevated miR-146a expression could increase the risk of cardiac disease/event in RA patients. Herein, we presume that elevated miR-146a may have no effect on increasing the risk of cardiac disease/event in RA patients.

Iguratimod is a promising DMARD with good potential to be widely used in RA management. Recent evidence shows that iguratimod boosts RA remission by diminishing pro-inflammatory processes and balancing the immune responses, interestingly, it also protects the bones from erosion, which is a huge advantage compared with other DMARDs or NSAIDs (35-38). In the clinical setting, iguratimod presents with good efficiency in RA management. A previous retrospective cohort study highlights that iguratimod achieves decreased retention rate, indicating the incidence of relapse and AEs, compared to salazosulfapyridine in RA patients (39). Another cohort study illustrates that iguratimod alone and combination of Iguratimod with methotrexate are both effective in RA patients after 3 years of treatment, presenting as the sustained reduction of disease

activity (40). Additionally, there is a retrospective cohort study reports that in RA patients with unsatisfying response to biological DMARDs, using iguratimod as an add-on therapeutic markedly reduces the disease activity score 28-erythrocyte sedimentation rate (DAS28-ESR) and the power Doppler score (a semi-quantitive score indicating the blood flow signal in joints) (41). As for the molecular mechanisms of iguratimod in alleviating inflammation and balancing immunity in RA, it has been illuminated that iguratimod reduces citrullinated proteins and peptidylarginine deiminases 2/4 in a dose-dependent way in neutrophils from RA patients (35). And a prior study reveals that iguratimod decreases the expression of biomarkers reflecting bone formation in serum of RA patients, which is a mechanism that could promote bone formation (42). In addition, there is a study reporting that iguratimod, methotrexate and their combination use all suppress the secretion of receptor activator of NF-κB ligand (RANKL), the elevation of which stimulates the bone erosion, in RA-FLS (43). Furthermore, thanks to the development in the technology of RNA sequencing, increasing miRNAs are found to play a regulatory role in the processes of RA therapy, however, there is still no report illuminating the interactions between iguratimod and miRNAs in RA. Therefore, considering that iguratimod is a MIF inhibitor, and more importantly, miR-146a is not only a mediator of immune and inflammatory responses but also a modulator of MIF expression, we investigated the interactions between iguratimod and miR-146a in RA-FLS in this study (18). We found that *in vitro*, iguratimod reduced cell viability in a dose-dependent manner, and inhibited cell proliferation, migration, invasion and inflammation, while it promoted apoptosis via upregulating miR-146a and downregulating its downstream gene IRAK1 as well as downstream pathway TRAF6/JNK1 in RA-FLS.

Iguratimod also exhibits good therapeutic effect in experiments conducted in animal models of inflammatory and immune diseases. For instance, a study shows that iguratimod represses paw swelling, protects the bone and cartilage from erosion, as well as reduces pro-inflammatory cytokines expressions in CIA rat model (44). Another study reveals that in the rat model of neuropathic pain, which is conducted to simulate the pain in RA, iguratimod relieves the neuropathic pain through a mechanism of repressing the allodynic effect (45). A previous study illustrates that iguratimod suppresses arthritic inflammation and reduces the IL-17 signaling in synovium tissue collected from CIA rat (41). In our study, for the purpose of verifying the *in vitro* results, we further conducted experiments *in vivo*, which revealed that:

a. inhibition of miR-146a elevated systemic arthritis score, and enhanced pro-inflammatory cytokines, IRAK1 expression as well as TRAF6/JNK1 pathway, while suppressed cell apoptosis in synovial tissue of CIA rat model;

b. Iguratimod decreased systemic arthritis score, and reduced pro-inflammatory cytokines while enhanced cell apoptosis in synovial tissue of CIA rat model by upregulating miR-146a and repressing IRAK1 expression and TRAF6/JNK1 pathway.

In conclusion, iguratimod ameliorates RA progression through regulating miR-146a mediated IRAK1 expression and TRAF6/JNK1 pathway.

References

1. SMOLEN JS, ALETAHA D, MCINNES IB: Rheumatoid arthritis. *Lancet* 2016; 388: 2023-38.
2. CROIA C, BURSI R, SUTERA D, PETRELLI F, ALUNNO A, PUXEDDU I: One year in review 2019: pathogenesis of rheumatoid arthritis. *Clin Exp Rheumatol* 2019; 37: 347-57.
3. JUNG N, BUEB JL, TOLLE F, BRECHARD S: Regulation of neutrophil pro-inflammatory functions sheds new light on the pathogenesis of rheumatoid arthritis. *Biochem Pharmacol* 2019; 165: 170-80.
4. MCINNES IB, SCHETT G: Pathogenetic insights from the treatment of rheumatoid arthritis. *Lancet* 2017; 389: 2328-37.
5. LI J, BAO J, ZENG J, YAN A, ZHAO C, SHU Q: Iguratimod: a valuable remedy from the Asia Pacific region for ameliorating autoimmune diseases and protecting bone physiology. *Bone Res* 2019; 7: 27.
6. DUAN XW, ZHANG XL, MAO SY, SHANG JJ, SHI XD: Efficacy and safety evaluation of a combination of iguratimod and methotrexate therapy for active rheumatoid arthritis patients: a randomized controlled trial. *Clin Rheumatol* 2015; 34: 1513-9.
7. OKAMURA K, YONEMOTO Y, SUTO T, OKURA C, TAKAGISHI K: Efficacy at 52 weeks of daily clinical use of iguratimod in patients with rheumatoid arthritis. *Mod Rheumatol* 2015; 25: 534-9.
8. OKAMURA K, YONEMOTO Y, OKURA C, KOBAYASHI T, TAKAGISHI K: Efficacy of the clinical use of iguratimod therapy in patients with rheumatoid arthritis. *Mod Rheumatol* 2015; 25: 235-40.
9. SHUKLA GC, SINGH J, BARIK S: MicroRNAs: processing, maturation, target recognition and regulatory functions. *Mol Cell Pharmacol* 2011; 3: 83-92.
10. LIM LP, GLASNER ME, YEKTA S, BURGE CB, BARTEL DP: Vertebrate microRNA genes. *Science* 2003; 299: 1540.
11. TAGANOV KD, BOLDIN MP, CHANG KJ, BALTIMORE D: NF-kappaB-dependent induction of microRNA miR-146, an inhibitor targeted to signaling proteins of innate immune responses. *Proc Natl Acad Sci USA* 2006; 103: 12481-6.
12. NAHID MA, PAULEY KM, SATOH M, CHAN EK: miR-146a is critical for endotoxin-induced tolerance: implication in innate immunity. *J Biol Chem* 2009; 284: 34590-9.
13. LABBAYE C, TESTA U: The emerging role of MIR-146A in the control of hematopoiesis, immune function and cancer. *J Hematol Oncol* 2012; 5: 13.
14. NAKASA T, SHIBUYA H, NAGATA Y, NIIMOTO T, OCHI M: The inhibitory effect of microRNA-146a expression on bone destruction in collagen-induced arthritis. *Arthritis Rheum* 2011; 63: 1582-90.
15. LI X, GIBSON G, KIM JS *et al*.: MicroRNA-146a is linked to pain-related pathophysiology of osteoarthritis. *Gene* 2011; 480: 34-41.
16. FU HX, FAN XP, LI M, LIU MJ, SUN QL: MiR-146a relieves kidney injury in mice with systemic lupus erythematosus through regulating NF-kappaB pathway. *Eur Rev Med Pharmacol Sci* 2019; 23: 7024-32.
17. REBANE A, RUNNEL T, AAB A *et al*.: MicroRNA-146a alleviates chronic skin inflammation in atopic dermatitis through suppression of innate immune responses in keratinocytes. *J Allergy Clin Immunol* 2014; 134: 836-47 e11.
18. WANG WM, LIU JC: Effect and molecular mechanism of mir-146a on proliferation of lung cancer cells by targeting and regulating MIF gene. *Asian Pac J Trop Med* 2016; 9: 806-11.
19. CHEN Y, XIAN PF, YANG L, WANG SX: MicroRNA-21 Promotes proliferation of fibroblast-like synoviocytes through mediation of NF-kappaB nuclear translocation in a rat model of collagen-induced rheumatoid arthritis. *Biomed Res Int* 2016; 2016: 9279078.
20. GAO J, ZHOU XL, KONG RN, JI LM, HE LL, ZHAO DB: microRNA-126 targeting PIK3R2 promotes rheumatoid arthritis synovial fibroblasts proliferation and resistance to apoptosis by regulating PI3K/AKT pathway. *Exp Mol Pathol* 2016; 100: 192-8.
21. CHEN Y, WU Z, YUAN B, DONG Y, ZHANG L, ZENG Z: MicroRNA-146a-5p attenuates irradiation-induced and LPS-induced hepatic stellate cell activation and hepatocyte apoptosis through inhibition of TLR4 pathway. *Cell Death Dis* 2018; 9: 22.
22. ROOS J, ENLUND E, FUNCKE JB *et al*.:

miR-146a-mediated suppression of the inflammatory response in human adipocytes. *Sci Rep* 2016; 6: 38339.
23. CHEN Y, ZENG Z, SHEN X, WU Z, DONG Y, CHENG JC: MicroRNA-146a-5p negatively regulates pro-inflammatory cytokine secretion and cell activation in lipopolysaccharide stimulated human hepatic stellate cells through inhibition of Toll-like receptor 4 signaling pathways. *Int J Mol Sci* 2016; 17.
24. BRAND DD, LATHAM KA, ROSLONIEC EF: Collagen-induced arthritis. *Nat Protoc* 2007; 2: 1269-75.
25. YOO SA, PARK BH, PARK GS *et al*.: Calcineurin is expressed and plays a critical role in inflammatory arthritis. *J Immunol* 2006; 177: 2681-90.
26. LAW ST, TAYLOR PC: Role of biological agents in treatment of rheumatoid arthritis. *Pharmacol Res* 2019; 150: 104497.
27. HONG H, YANG H, XIA Y: Circulating miR-10a as predictor of therapy response in rheumatoid arthritis patients treated with methotrexate. *Curr Pharm Biotechnol* 2018;19: 79-86.
28. STICKEL N, HANKE K, MARSCHNER D *et al*.: MicroRNA-146a reduces MHC-II expression via targeting JAK/STAT signaling in dendritic cells after stem cell transplantation. *Leukemia* 2017; 31: 2732-41.
29. LULY FR, LEVEQUE M, LICURSI V *et al*.: MiR-146a is over-expressed and controls IL-6 production in cystic fibrosis macrophages. *Sci Rep* 2019; 9: 16259.
30. FEI Y, CHAULAGAIN A, WANG T *et al*.: MiR-146a down-regulates inflammatory response by targeting TLR3 and TRAF6 in Coxsackievirus B infection. *RNA* 2020; 26: 91-100.
31. QU X, WANG N, CHENG W, XUE Y, CHEN W, QI M: MicroRNA-146a protects against intracerebral hemorrhage by inhibiting inflammation and oxidative stress. *Exp Ther Med* 2019; 18: 3920-28.
32. AMROUCHE L, YOU S, SAUVAGET V *et al*.: MicroRNA-146a-deficient mice develop immune complex glomerulonephritis. *Sci Rep* 2019; 9: 15597.
33. BERTOLET G, KONGCHAN N, MILLER R *et al*.: MiR-146a wild-type 3' sequence identity is dispensable for proper innate immune function in vivo. *Life Sci Alliance* 2019; 2.
34. PAN JA, TANG Y, YU JY *et al*.: miR-146a attenuates apoptosis and modulates autophagy by targeting TAF9b/P53 pathway in doxorubicin-induced cardiotoxicity. *Cell Death Dis* 2019; 10: 668.
35. LI B, LI P, BI L: Iguratimod dose dependently inhibits the expression of citrullinated proteins and peptidylarginine deiminases 2 and 4 in neutrophils from rheumatoid arthritis patients. *Clin Rheumatol* 2020; 39: 899-907.
36. ISHIKAWA K, ISHIKAWA J: Iguratimod, a synthetic disease modifying anti-rheumatic drug inhibiting the activation of NF-kappaB and production of RANKL: Its efficacy, radiographic changes, safety and predictors over two years' treatment for Japanese rheumatoid arthritis patients. *Mod Rheumatol* 2019; 29: 418-29.
37. SONG J, LIU H, ZHU Q *et al*.: T-614 Promotes Osteoblastic Cell Differentiation by Increasing Dlx5 Expression and Regulating the Activation of p38 and NF-kappaB. *Biomed Res Int* 2018; 2018: 4901591.
38. WU YX, SUN Y, YE YP *et al*.: Iguratimod prevents ovariectomyinduced bone loss and suppresses osteoclastogenesis via inhibition of peroxisome proliferatoractivated receptor-gamma. *Mol Med Rep* 2017; 16: 8200-08.
39. NOZAKI Y, INOUE A, KINOSHITA K, FUNAUCHI M, MATSUMURA I: Efficacy of iguratimod vs. salazosulfapyridine as the first-line csDMARD for rheumatoid arthritis. *Mod Rheumatol* 2019: 1-10.
40. SUTO T, YONEMOTO Y, OKAMURA K *et al*.: The three-year efficacy of iguratimod in clinical daily practice in patients with rheumatoid arthritis. *Mod Rheumatol* 2019; 29: 775-81.
41. LUO Q, SUN Y, LIU W *et al*.: A novel disease-modifying antirheumatic drug, iguratimod, ameliorates murine arthritis by blocking IL-17 signaling, distinct from methotrexate and leflunomide. *J Immunol* 2013; 191: 4969-78.
42. WANG X, MA C, LI P, ZHAO F, BI L: Effects of iguratimod on the levels of circulating regulators of bone remodeling and bone remodeling markers in patients with rheumatoid arthritis. *Clin Rheumatol* 2017; 36: 1369-77.
43. WANG XT, LI P, XU TS, DING R, ZHANG X, BI LQ: Effect of iguratimod and methotrexate on RANKL and OPG expression in serum and IL-1beta-induced fibroblast-like synoviocytes from patients with rheumatoid arthritis. *Cell Mol Biol* 2016; 62: 44-50.
44. DU F, LU LJ, FU Q *et al*.: T-614, a novel immunomodulator, attenuates joint inflammation and articular damage in collagen-induced arthritis. *Arthritis Res Ther* 2008; 10: R136.
45. MORIMOTO K, MIURA A, TANAKA K: Anti-allodynic action of the disease-modifying anti-rheumatic drug iguratimod in a rat model of neuropathic pain. *Inflamm Res* 2017; 66: 855-62.